Mon. Not. R. Astron. Soc. **282,** 1321–1329 (1996)

Optical constants of cosmic carbon analogue grains – I. Simulation of clustering by a modified continuous distribution of ellipsoids

V. G. Zubko,[1]★† V. Mennella,[2]† L. Colangeli[2]† and E. Bussoletti[3]†

[1]*Institute of Astronomy, N. Copernicus University, Chopina 12/18, Pl-87-100 Toruń, Poland*
[2]*Osservatorio Astronomico di Capodimonte, via Moiariello 16, I-80131 Napoli, Italy*
[3]*Istituto di Fisica Sperimentale, Istituto Universitario Navale, via A. De Gasperi 5, I-80125 Napoli, Italy*

Accepted 1996 June 7. Received 1996 May 22; in original form 1996 January 9

ABSTRACT

The first results on the optical constants of three different amorphous carbon samples, possible analogues of interstellar and circumstellar dust grains, are presented. They have been deduced from recent laboratory data, making use of the Kramers–Kronig approach. It is shown that the physically correct simulation of clustering by the traditional 'CDE' model is not applicable here. A modified CDE (MCDE) model is proposed and used in the present calculations. The MCDE model allows one to take into account the effect of percolation of the analysed amorphous carbon clusters through the parameter g_o, interpreted as a percolation strength. The intervals of the probable MCDE models (g_o) have been chosen on the basis of the relevant estimates of Stognienko, Henning & Ossenkopf for the cluster–cluster aggregation (CCA) and particle–cluster aggregation (PCA) models. The 'optimal' percolation strengths and optical constants have been derived by using a least-squares procedure.

Key words: stars: carbon – circumstellar matter – dust, extinction.

1 INTRODUCTION

Much evidence has been accumulated regarding carbon as an important constituent of cosmic grains. There is an estimate of 60–70 per cent depletion of carbon from the gas phase (Cardelli et al. 1993). Graphite, SiC and diamond grains of probable interstellar origin have been found in meteorites (Anders & Zinner 1993; Ott 1993). Modelling of interstellar extinction curves and, especially, of the 217.5-nm hump requires graphite to be the principal carbon component with possible small amounts of amorphous carbon (Kim, Martin & Hendry 1994; Aanestad 1995). However, this leads to the problem of large graphite grains: the well-known grain size distributions of Mathis, Rumpl & Nordsieck (1977) and Kim et al. (1994) contain noticeable amounts of graphite grains with radii > 0.1 μm. It is not clear what is a suitable astronomical environment to produce such grains.

On the other hand, many data from laboratory simulations of cosmic dust analogues appear to provide evidence in favour of various forms of amorphous carbon rather than graphite grains (Czyzak & Santiago 1973; Stephens 1980; Donn et al. 1981; Bussoletti et al. 1987; Colangeli et al. 1995). Hecht (1986) and later Sorrell (1990) have proposed that the major part of interstellar carbon dust is concentrated in amorphous grains, mainly expelled from the atmospheres of carbon-rich asymptotic giant branch (AGB) stars, with small amounts of tiny hydrogen-free graphitic grains (5–7 nm) formed from the amorphous ones as a result of their dehydrogenation. Physically the dehydrogenation may be caused by shocks, UV irradiation or cosmic rays. It is the population of graphitic grains that may explain the 217.5-nm feature.

A wide variety of amorphous carbons are produced in the laboratory. They mainly differ in terms of density, sp^2/sp^3 ratio and amount of hydrogen. The sp^2 sites form graphitic clusters embedded in an sp^3 bonded matrix. During recent

★On leave from the Main Astronomical Observatory, National Academy of Sciences, Kiev, Ukraine.
†E-mail: zubko@astri.uni.torun.pl (VGZ);
mennella@astrna.na.astro.it (VM);
colangeli@astrna.na.astro.it (LC);
bussoletti@nava1.uninav.it (EB)

years, progress has been made in laboratory investigation of cosmic carbon analogue grains. Mennella et al. (1995a, b) have shown that the UV extinction produced by carbon grains strongly depends on the electronic properties and dimensions of the sp^2 clusters. The important role of hydrogen in the evolution of carbon grains has been proved (Blanco et al. 1991, 1993; Colangeli et al. 1993; Mennella et al. 1995a). It was shown that the amorphous carbon grains produced in hydrogen atmospheres do not exhibit a distinct feature between 200 and 300 nm (Blanco et al. 1991), whereas during annealing an effusion of hydrogen from the grains occurs; a UV peak appears and its position shifts from 194 to 259 nm as the annealing temperature increases from 250°C to 800°C (Mennella et al. 1995a). Such behaviour shows that the presence of hydrogen favours the sp^3 bonds. The hydrogen effusion promotes an increase in number and dimension of sp^2 clusters, and their contribution becomes significant in grain extinction. It is now possible to identify precisely the relation between the extinction properties of a given amorphous carbon sample measured in the laboratory and its internal structure.

Recently, data from new extinction measurements of various amorphous carbon samples ranging from 0.04–0.05 μm to 2 mm have been published (Colangeli et al. 1995). To model the cosmic carbon grains, however, the appropriate optical constants are needed. The often-used Rouleau & Martin (1991) optical constants of amorphous carbon have mainly been derived from the previous data given by Bussoletti et al. (1987). However, the data from new extinction measurements by Colangeli et al. (1995) are essentially extended towards the extreme-UV (EUV) up to 0.04 μm (from the 0.1 μm of the old data) and up to 2 mm (from 300 μm) in the far-IR. Therefore we are performing a comprehensive theoretical study of the optical constants of various amorphous carbon materials on the basis of new extinction laboratory data, the Kramers–Kronig relations, and state-of-the-art theoretical and computational tools in cluster modelling, such as the 'effective medium' theories (Ossenkopf 1991; Stognienko, Henning & Ossenkopf 1995), the discrete dipole approximation (Draine 1988; Draine & Flatau 1994), and the discrete multipole method (Hamid, Ciric & Hamid 1990; Hinsen & Felderhof 1992).

The objective of the present explanatory paper is twofold. Our first aim is to describe our basic theoretical approach. Our second goal is to present the optical constants of amorphous carbon materials (ACAR, BE and ACH2 samples: see Section 2) resulting from our preliminary calculations. It should be noted that the detailed morphological study of the above samples, including their elementary grain shape, structure and clustering, is now in progress, and consequently will be taken into account in future studies.

In the present work we have simulated the clustering effects using various continuous distributions of randomly oriented ellipsoids (hereafter CDE and CDE-like models). The validity of such an approach has already been shown by Rouleau & Martin (1991). Section 2 contains a short description of the available physical properties of the amorphous carbon samples involved in the analysis. The details of our theoretical approach are the subject of Section 3. The results are presented and discussed in Section 4. The conclusions are summarized in Section 5.

2 AMORPHOUS CARBON SAMPLES

We have considered the results of measurements for amorphous carbon grains produced under the following conditions:

(i) arc discharge between amorphous carbon electrodes in an Ar atmosphere at 10 mbar (ACAR sample);
(ii) arc discharge between the same type of electrodes in an H_2 atmosphere at 10 mbar (ACH2 sample);
(iii) burning of benzene in air under normal conditions (BE sample).

Spectroscopic measurements were carried out in transmission. The experimental set-up and sample preparation were extensively described by, e.g., Colangeli et al. (1993, 1995) and Mennella et al. (1995a).

The measurements were performed by depositing calibrated dust amounts on to spectroscopic grade substrates, transparent in different spectral ranges, or by embedding the grains in matrices, by means of standard pellet techniques. In all cases, the sample mass was measured by using a microbalance (± 1 μg accuracy). Since, for all the kinds of carbon analysed, the extinction coefficient decreases as the wavelength increases, different masses were needed according to the spectral range considered in order to record spectra with the best signal-to-noise ratio.

Amorphous carbon grains condense in chain-like structures containing single grains with typical spheroidal shape. In addition, grains are mostly aggregated in clusters containing some three to five individual grains. In turn, such clusters are linked together in a necklace–fractal structure. The average radius of the grains is 5–6 nm for the ACAR and ACH2 samples and about 15 nm for the BE sample.

The extinction coefficients per unit mass that we used for the present study are shown in Fig. 1. It should be noted that all of these data correspond to grains simply sitting *on* a substrate, and are corrected to take into account the matrix effect.

Emphasis should be placed on the homogeneity of the extinction data under analysis, as they have been obtained for the same samples and under the same laboratory conditions. In addition, these data extend from the EUV to the

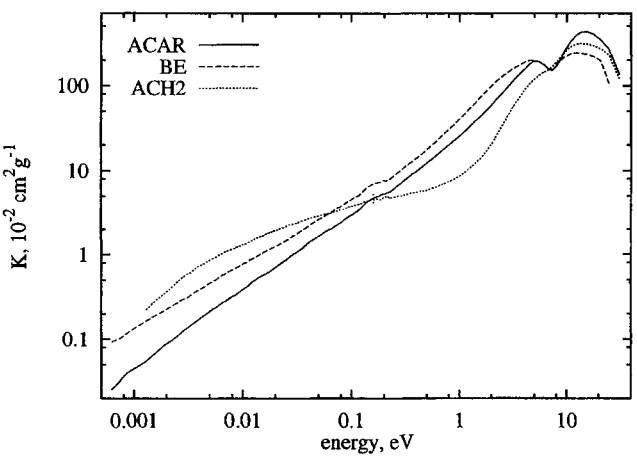

Figure 1. Extinction coefficients of the analysed samples.

mm region, and therefore cover the greatest range suitable for a theoretical investigation aimed at extracting appropriate optical constants.

3 THEORETICAL APPROACH

3.1 Constraints on the dielectric function

Our goal was to derive the dielectric function $\varepsilon=\varepsilon_r+i\varepsilon_i$, where ε_r and ε_i are the real and imaginary parts, respectively, and the optical constants n and k (the components of the complex refractive index $m=n+ik$, $\varepsilon=m^2$) of an amorphous carbon grain sample as a function of energy E from the extinction coefficient K measured in the energy interval $[E_{min}, E_{max}]$. Since the K-data that we used are free from the matrix effects, we define the dielectric function ε relative to the 'vacuum' assumed as a surrounding medium. The method that we used is mainly based on the works of Ku & Felske (1986), Rouleau & Martin (1991) and Laor & Draine (1993).

We looked for the dielectric function ε that obeyed the following general constraints.

(i) The fundamental Kramers–Kronig relations (Landau, Lifshits & Pitaevskii 1984) have to be satisfied:

$$\varepsilon_r(E)=1+\frac{2}{\pi}P\int_0^\infty \frac{\tilde{E}\varepsilon_i(\tilde{E})}{\tilde{E}^2-E^2}\,d\tilde{E}, \tag{1}$$

$$\varepsilon_i(E)=-\frac{2}{\pi}EP\int_0^\infty \frac{\varepsilon_r(\tilde{E})}{\tilde{E}^2-E^2}\,d\tilde{E}, \tag{2}$$

where P denotes the Cauchy principal value integral.

(ii) The initial extinction coefficient $K(E)$ has to be recovered from $\varepsilon(E)$.

In addition, we applied a few specific constraints, taking into account the properties of the amorphous carbon grains.

(i) The sum rule for the effective number of electrons per carbon atom must hold true:

$$N_{eff}=\lim_{E\to\infty}\frac{2m_e m_c}{\rho e^2 h^2}\int_0^E \tilde{E}\varepsilon_i(\tilde{E})\,d\tilde{E}=6, \tag{3}$$

where m_e (m_c) is the mass of an electron (a carbon atom), e is the elementary charge of the electron, h is the Planck constant and ρ is the mass density of the grain material.

(ii) The static real part of the dielectric function has to be positive: $\varepsilon_r(E\to 0)>0$.

The last condition is based on the experimental measurements of the optical gap of the amorphous samples under analysis. It is equal to 0.52 eV for ACAR, 0.15 eV for BE (Mennella et al. 1995c) and 1.32 eV for ACH2 (Mennella et al. 1995b). So we may conclude that all our samples are semiconductors rather than metals.

3.2 Models of the polarizability of a grain

We choose the function $A(E)$ of Ku & Felske (1986) as an intermediate function to evaluate the optical constants of the amorphous carbon samples, for the following reasons.

(i) For grains in the Rayleigh limit (which is mainly the case in our analysis), this function may be physically interpreted as a dipole polarizability. Consequently, its functional dependence on ε may be found by assuming a grain shape and structure, and it is useful for the evaluation of ε.

(ii) Like ε, this function also satisfies the Kramers–Kronig relations (Ku & Felske 1986):

$$A_r(E)=\frac{2}{\pi}P\int_0^\infty \frac{\tilde{E}A_i(\tilde{E})}{\tilde{E}^2-E^2}\,d\tilde{E}, \tag{4}$$

$$A_i(E)=-\frac{2}{\pi}EP\int_0^\infty \frac{A_r(\tilde{E})}{\tilde{E}^2-E^2}\,d\tilde{E}, \tag{5}$$

(iii) There is a simple relation connecting the imaginary part of the polarizability A_i with the extinction coefficient K obtained from laboratory measurements (Ku & Felske 1986):

$$A_i(E)=\frac{hc}{2\pi}\rho\frac{K(E)}{E}. \tag{6}$$

Of course, it is strictly valid for grains in the Rayleigh limit. The real part A_r may then be found from the Kramers–Kronig relation (4).

We note the difference of a factor of 3 between the polarizability A definitions used by Rouleau & Martin (1991) and Ku & Felske (1986). All of our formulae containing A correspond to Rouleau & Martin's notation. It directly reflects the physical meaning of A as the total dipole moment of a grain per unit grain volume and per unit tension of the applied electric field (Bohren & Huffman 1983).

Rouleau & Martin (1991) have investigated the effects of grain shape and clustering on the optical constants of amorphous carbon grains, and found them to be significant. They have derived the optical constants for two amorphous carbon samples, AC1 and BE1, on the basis of the CDE shape distribution and of 'optimized' models with grain agglomeration: homogeneous aggregation (HA) and fractal clusters (FC). The same authors found the results of aggregated models to be qualitatively mimicked by the simpler CDE model. However, our attempts to apply the CDE model to the analysis of the extinction data from Colangeli et al. (1995) were without success for the BE and ACH2 samples, mainly because of the breakdown of the condition $\varepsilon_r(E\to 0)>0$. The same result was obtained by applying the HA and FC models with both single spheres and CDE. The detailed modelling of clustering will be presented in forthcoming papers. In the present work we introduce some CDE-like forms of shape distributions which allowed us to simulate the clustering of the samples with greatly enhanced extinction where the CDE model given by Bohren & Huffman (1983) fails.

The simplest dependence $A(\varepsilon)$ may be written for a Rayleigh sphere (Bohren & Huffman 1983):

$$A_{rs}(\varepsilon)=3\frac{\varepsilon-1}{\varepsilon+2}. \tag{7}$$

Evidently, the maximal value of $\mathrm{Re}(A_{rs})$ in the static limit $\varrho \to 0$ cannot exceed 3. However, our calculations show that for all samples $A_r(E \to 0) \gtrsim 9$. Therefore the single-sphere model is not appropriate, in agreement with the known grain agglomeration.

The $A(\varepsilon)$ dependence is defined by the grain structure. In particular, for homogeneous ellipsoids (Bohren & Huffman 1983),

$$\tilde{A}_{el}(\varepsilon, L) = \frac{\varepsilon - 1}{1 + L(\varepsilon - 1)}, \tag{8}$$

where L is a geometrical factor ranging from 0 to 1. For a sphere $L = 1/3$ and for ellipsoids there are three factors L_1, L_2 and L_3 fulfilling the relation $L_1 + L_2 + L_3 = 1$. Thus, averaging over an ensemble of randomly oriented and shape-distributed ellipsoids, we may write

$$A_{el}(\varepsilon) = \frac{1}{3} \sum_{i=1}^{3} \iint_{\Delta} P(L_1, L_2) \tilde{A}_{el}(\varepsilon, L_i)\, \mathrm{d}L_1\, \mathrm{d}L_2, \tag{9}$$

where the shape distribution function $P(L_1, L_2)$ is defined on the triangular region $\Delta\ \{L_1 = [0, 1], L_2 = 1 - L_1\}$ (Bohren & Huffman 1983) and is normalized to 1 on the Δ-region. If we assume a homogeneous shape distribution of *all* possible forms of ellipsoids (CDE), then $P(L_1, L_2) = 2$ and we obtain (Bohren & Huffman 1983)

$$A_{cde}(\varepsilon) = 2\left(\frac{\varepsilon \ln \varepsilon}{\varepsilon - 1} - 1\right). \tag{10}$$

The CDE model reproduces the effects of grain clustering because it accounts for the extreme forms with L around 0, corresponding to some orientations of cylinders and discs (Rouleau & Martin 1991). However, in the CDE model the probability of these shapes and the probability of, say, spheres are the same. Actually, our simulation of the agglomerated structures (Section 4) shows that the contribution of the extreme forms should be higher than in the CDE model. Note the arbitrariness of the traditional CDE model used in the previous papers by Rouleau & Martin (1991) and Preibisch et al. (1993) when the same constant probability is assigned for all possible shapes. It seems to be very unrealistic. Recently, Stognienko et al. (1995) have analysed the optical properties of the model clustered grains taken as a two-phase composite system by using the so-called spectral representation. The spectral function introduced by this representation exclusively contains the geometric information about the system. Stognienko et al. (1995) have shown that, in order to describe the percolation of the clusters, the spectral function may be decomposed into two parts, accounting for the contributions of the extreme mode and the rest of the forms, respectively. Starting from the analogy between the abovementioned spectral function and the shape distribution function $P(L_1, L_2)$, we have considered a few modified homogeneous shape distributions aimed at describing the percolated clusters of amorphous carbon grains. In the *externally* restricted distribution of ellipsoids (ERCDE), $P(L_1, L_2)$ is constant on the triangle region $\Delta'\ \{L_1 = [L_a, L_b],\ L_2 = [L_a, L_a + L_b - L_1]\}$ and vanishes on the remainder of the Δ-region, Δ''. In contrast, in the *internally* restricted distribution of ellipsoids (IRCDE), the function $P(L_1, L_2)$ is equal to zero on the region Δ' and constant on Δ''. The characteristic geometrical factors of ERCDE and IRCDE are

$$L_a = \tfrac{1}{3}(1 - \delta), \qquad L_b = \tfrac{1}{3}(1 + 2\delta), \tag{11}$$

where the only parameter of the models, δ, is in the range 0 to 1. Thus the ERCDE allows us to cut off the ellipsoids with the largest deviation from a sphere, whereas the IRCDE takes into consideration just these forms. By substituting the shape distributions $P(L_1, L_2) = 2/\delta^2$ (ERCDE) and $P(L_1, L_2) = 2/(1 - \delta^2)$ (IRCDE) into (9) and by integrating, we obtain

$$A_{ercde}(\varepsilon, \delta) = \frac{2}{\delta^2}\left[\frac{1}{\tilde{A}_{el}(\varepsilon, L_b)} \ln \frac{\tilde{A}_{el}(\varepsilon, L_a)}{\tilde{A}_{el}(\varepsilon, L_b)} - \delta\right], \tag{12}$$

$$A_{ircde}(\varepsilon, \delta) = \frac{A_{cde}(\varepsilon) - \delta^2 A_{ercde}(\varepsilon, \delta)}{1 - \delta^2}. \tag{13}$$

In the limit of small δ, the region Δ' degenerates into the point with $L_1 = L_2 = 1/3$, and the ERCDE reduces to the case of a Rayleigh sphere:

$$\lim_{\delta \to 0} A_{ercde}(\varepsilon, \delta) = A_{rs}(\varepsilon) \tag{14}$$

whereas the IRCDE transforms into the CDE. In turn, the CDE is a limiting form of the ERCDE if $\delta \to 1$ and $\Delta' \equiv \Delta$. However, when $\delta \to 1$ the IRCDE transforms into a new, 'extreme' distribution of ellipsoids (EDE):

$$A_{ede}(\varepsilon) = \tfrac{1}{3}(\varepsilon - 1 + 2 \ln \varepsilon), \tag{15}$$

containing the extreme forms around $L = 0$.

We next introduced a more complicated shape distribution, the *step* distribution of ellipsoids (SDE), where $P(L_1, L_2)$ assumes two constant values on the triangle regions Δ' and Δ''. It is natural to define a new parameter of the SDE, g_o, as the fraction of ellipsoids occupying the region Δ''. Then the fraction of ellipsoids contained in the region Δ'' is $1 - g_o$. By substituting the relevant values of $P(L_1, L_2)$ for the SDE into (9) and by integrating, we have

$$A_{sde}(\varepsilon, \delta, g_o) = g_o A_{ircde}(\varepsilon, \delta) + (1 - g_o) A_{ercde}(\varepsilon, \delta). \tag{16}$$

If we finally go to the limit $\delta \to 1$ in (16) we obtain the *modified* CDE or MCDE:

$$A_{mcde}(\varepsilon, g_o) = g_o A_{ede}(\varepsilon) + (1 - g_o) A_{cde}(\varepsilon). \tag{17}$$

Thus, in the derived distribution of ellipsoids, the component responsible for percolation, related to the shape factor $L = 0$, is separated from the other forms, which are uniformly distributed. By analogy with the spectral representation, the parameter g_o may be interpreted as the percolation strength. Of course, as with the conventional CDE, the new MCDE shape distribution suffers from the arbitrariness of the uniform probabilities of all forms with $L > 0$. However, at present, we are unable to estimate the actual spectral function of our amorphous carbon samples. On the other hand, since at very low energies the extinction of the amorphous carbon clusters depends only on the absolute magnitude of the spectral function (Stognienko et al. 1995), there is no need to determine the detailed distribution.

We used the MCDE shape distribution in our calculations and found it useful to generalize the classical CDE and

to account for the grain shapes simulating the enhanced extinction at low energies.

It should be noted that all of the abovementioned CDE-like models are strictly valid if the elementary grains, the constituents of clusters, are quite small (Rayleigh particles). However, we have analysed the data for measurements in the EUV at wavelengths $\lambda \gtrsim 40$ nm for grain sizes 5–6 nm where the size parameter $\alpha \lesssim 1$. Therefore an application of our models to derive the dielectric function in the UV has to be considered an extrapolation. The accuracy of this extrapolation may be deduced only by more detailed models which are beyond the scope of the present paper.

3.3 Practical calculation of the polarizability

To evaluate $A_r(E)$ by means of equation (4), $A_i(E)$ has to be known in the whole energy range $[0, \infty]$. In our case, $A_i(E)$ was obtained from equation (6) for energies in the range $[E_{min}, E_{max}]$, where K is measured, and by extrapolation in the intervals $[0, E_{min}]$ and $[E_{max}, \infty]$.

To estimate A_i in the low-energy interval $[0, E_{min}]$, we have used a power law: $A_i \sim E^{\gamma}$. The values of γ have been chosen by power-law-approximating the far-IR segments of A_i in the energy intervals 0.0006–0.004 eV for ACAR and BE, and 0.0013–0.003 eV for ACH2, i.e. near the low-energy edges of the experimental data sets. We have tried to use energy intervals in which the power-law behaviour of A_i is distinct. Our choice seems to be satisfactory, except for ACAR: in this case there are some oscillations of A_i in the chosen energy interval, so that γ was obtained from the best power-law trend of A_i. We derived γ_{fit} equal to ~ 0.008 for ACAR, -0.224 for BE and 0.069 for ACH2.

It is well known that the theory predicts a linear dependence $A_i \sim E$ at very low energies for ellipsoidal grains of any nature having even a negligible amount of free electrons (Landau et al. 1984). However, this dependence was not observed up to the lowest energies of available measurements for all analysed samples. A turnover of γ to 1 at very low energies cannot be ruled out. We have studied the sensitivity of the final optical constants to the adopted values of γ_{fit} by dividing the interval $[0, E_{min}]$ into two parts: $[E_{int}, E_{min}]$, where we adopt γ_{fit} from the power-law approximation, and $[0, E_{int}]$, where we have tested various γ-values between γ_{fit} and 1. By varying the energy E_{int} we have found that for $E_{int} \lesssim 0.1E_{min}$ the optical constants derived for the energies from E_{min} up to E_{max} do not significantly depend on the adopted extrapolation of A_i in $[0, E_{int}]$, for the analysed values of γ. Such a result reflects the local character of the Kramers–Kronig relations used for the calculation of the optical constants.

To estimate the dielectric function ε and A_i at high energies, we have taken the imaginary part of the dielectric function ε_i in the X-ray region by following Laor & Draine (1993):

$$\varepsilon_i \approx \frac{hc}{2\pi m_c} \frac{\rho}{E} \sum_{nl} \sigma_{nl}(E), \tag{18}$$

where $\sigma_{nl}(E)$ is the gas-phase photoelectric absorption cross-section for the carbon atom, and the sum runs over the subshells nl of carbon. Equation (18) is valid for $E \gtrsim 100$ eV but may be used as reasonable approximation for $E \gtrsim 25$ eV (Laor & Draine 1993). There are two different methods to calculate the photoelectric absorption cross-section σ_{nl}. The first one is based on the empirical fitting formula of Laor & Draine (1993), whereas the second one gives the analytic fits to the partial Hartree–Dirac–Slater photoionization cross-sections for the ground-state shells of the carbon atom (Verner et al. 1993; Verner & Yakovlev 1995). The last method seems to be most accurate and, therefore, it has been used in our calculations.

With ε_i being defined, the real part ε_r was calculated using the Kramers–Kronig relation (1). Strictly, in order to apply equation (1) we need to know ε_i in the whole energy range $[0, \infty]$. However, at the initial zero-approximation step we only specified ε_i by equation (18) in the range 13 to 3500 eV. We next calculated ε_r with equation (1) in the range E_{max} (around 30 eV) to 1000 eV. In the next iteration, after the derivation of A and then of ε in the main energy region, we had ε_i already defined in the energy region from E_{min} to 3500 eV and were able to calculate ε_r at high energies with sufficient precision.

In order to estimate A_i at high energies we need to specify the structure of the grains. We have already noticed that the grain samples under analysis have a complicated structure, although elementary grains have a typical spheroidal shape (Colangeli et al. 1995). It should be noted that at energies $\gtrsim 30$ eV we face the problem of extinction corresponding to the size parameters $\alpha \gtrsim 1$, where no simple approach exists to calculate the optical properties of a complicated grain. We have decided to *estimate* A_i at high energies on the basis of the extinction efficiencies of spherical grains Q_{ext} which have been calculated by using the standard Mie theory (Bohren & Huffman 1983):

$$A_i(E) = \frac{3}{4} \frac{Q_{ext}(\alpha, E)}{\alpha}. \tag{19}$$

Note that the application of Mie theory is sufficient for our purposes since, based on the results of Stognienko et al. (1995), we may expect the shape effects to be small for the optical constants in the UV.

3.4 The main algorithm of the calculations

According to the points discussed in the previous section, our algorithm was based on the following steps.

(i) For energies in the range $[E_{min}, E_{max}]$, where the measurements of the extinction coefficient K are available, calculate $A_i(E)$ from equation (6).

(ii) Estimate A_i in the low-energy interval $[0, E_{min}]$, by using a power-law extrapolation: $A_i \sim E^{\gamma}$.

(iii) Estimate A_i at high energies: (a) calculate ε_i at high energies ($E > E_{max}$) from equation (18); take ε_i for $E \leq E_{max}$ from the last iteration; (b) calculate ε_i at high energies by using the Kramers–Kronig relation (1); (c) calculate A_i at high energies from equation (19).

(iv) For a specified parameter g_o calculate the dielectric function ε for energies in the range $[E_{min}, E_{max}]$ from the non-linear equation $A_{mcde}(\varepsilon, g_o) = A_{data}(E)$, where $A_{mcde}(\varepsilon, g_o)$ is defined by equation (17) and $A_{data}(E)$ is derived in the previous steps.

(v) For each E in the $[E_{min}, E_{max}]$ range, compare $\varepsilon(E)$ with its value in the previous iteration: if convergence to within an adopted precision is reached then step, else return to step (iii).

4 RESULTS

The application of the MCDE models for the Kramers–Kronig analysis has required the specification of the percolation strength g_o. It has turned out that physically plausible values of n and k are obtained for all the g_o values from 0 (CDE) to 1 (EDE) only for ACAR. In contrast, we have found that the MCDE models with $g_o < 0.006$ for BE and < 0.040 for ACH2 either diverge or lead to unphysical n and k, with a breakdown of the requirement $\varepsilon_r(E \to 0) > 0$. So, under these conditions, the traditional CDE model fails. As we have already mentioned, a detailed morphological study of ACAR, BE and ACH2 samples is in progress (Rotundi et al., in preparation). Therefore we have had to apply available models to reduce the interval of possible values of g_o. Despite the different sizes of grains, the general agglomeration structure looks similar for all the samples (Colangeli et al. 1995). This has given us an opportunity to apply a unified MCDE model to the analysis of all our samples. Stognienko et al. (1995) have theoretically studied the optical behaviour of dust aggregates in two limiting cases of the dust coagulation process, PCA (particle–cluster aggregation) and CCA (cluster–cluster aggregation), and estimated the upper limit of the percolation strengths g_o for the 'real' CCA and PCA clusters to be equal to 0.114 and 0.061, respectively. A comparison of images of the amorphous carbon samples by Colangeli et al. (1995) with those of the abovementioned clusters by Stognienko et al. (1995) shows that the structure of the samples looks like that of a CCA cluster. Therefore we have adopted the value 0.114 as an *upper* limit of the interval of the probable value of g_o. Since we lack any additional information about the possible *lower* limit of g_o for the CCA cluster, we have used for it the value 0.061, corresponding to the upper estimate of g_o for the PCA cluster.

To find the best MCDE model (g_o) and the corresponding optical constants for each sample, we have carried out a least-squares procedure by minimizing the following residual function:

$$\Phi(g_o) = \int_{0.061}^{0.114} \mathrm{d}\tilde{g}_o \int_{E_{min}}^{E_{max}} \mathrm{d}\tilde{E} \{A_i^{exp}(\tilde{E}) - A_i^{mcde}[\varepsilon(\tilde{E}, \tilde{g}_o), g_o]\}^2, \tag{20}$$

where the first integration is over the adopted set of MCDE models: $g_o = 0.061$–0.114. This interval has been chosen to be the same for all the samples, owing to their similar morphological structure. The integration over energy covers the whole region where the imaginary part of the polarizability A_i^{exp} may be directly deduced from the experimental data using equation (6). In equation (20) the dielectric function $\varepsilon(\tilde{E}, \tilde{g}_o)$ is calculated for each $\tilde{g}_o$ from $A_i^{exp}(\tilde{E})$ with the procedure described above. So the models that we obtained with such an approach at least uniformly deviate from the 'laboratory' A^{exp}. We have obtained the following 'optimal' values: $g_o = 0.086 \pm 0.001$ for ACAR, 0.085 ± 0.001 for BE and 0.083 ± 0.001 for ACH2; these are in good agreement with the g_o estimates of Stognienko et al. (1995). The similar values of the percolation strengths g_o confirm an initial assumption about the morphological similarity of the samples. The resultant optical constants for all the samples derived by using the 'optimal' MCDE models are displayed in Fig. 2 and are listed in Table 1. The energy range reflects the range of the extinction measurements.

As far as the probable errors of the derived optical constants are concerned, we note that, according to our procedure, they mainly stem from the uncertainties of the input extinction coefficient K, and the low-energy extrapolation of A_i. In fact, the influence of the errors of the numerical procedure may be made negligible by choosing an appropriately large number of energy points for evaluation of the Kramers–Kronig integrals, and the most demanding convergence criteria of the Newton–Raphson method used for resolution of non-linear equations. Some uncertainty is contributed by the high-energy approximation. However, we suppose it to be negligible with respect to the other uncertainties.

Since it is difficult to make direct estimates of errors, we

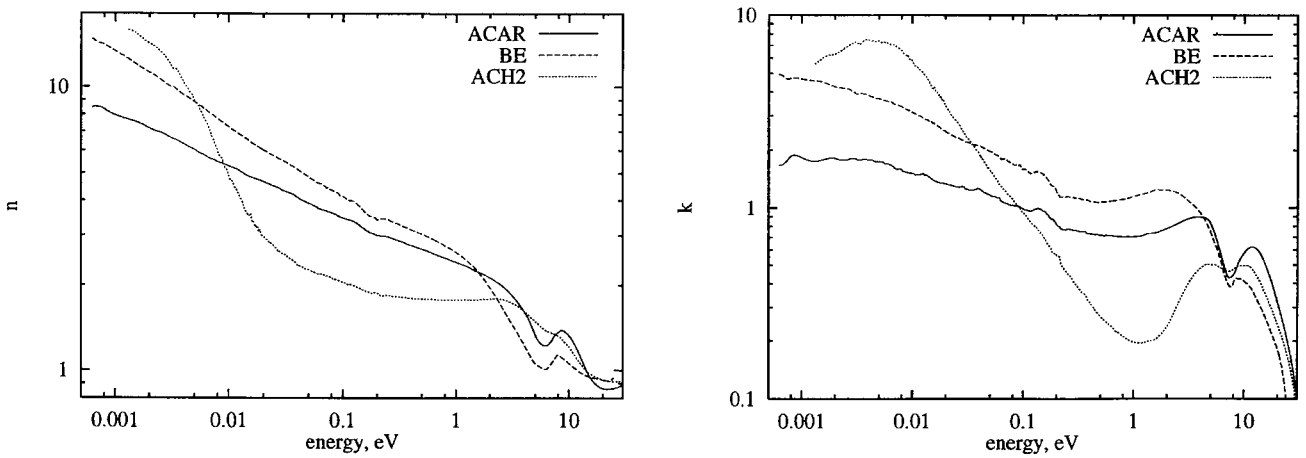

Figure 2. The final optical constants of the analysed amorphous carbon grains obtained with the 'optimal' MCDE models. The percolation strength, g_o, is 0.086 for ACAR, 0.085 for BE and 0.083 for ACH2.

Table 1. The optical constants for the materials examined.

	ACAR		BE		ACH2	
E, eV	n	k	n	k	n	k
6.208–4	8.470	1.668	14.735	4.940		
6.771–4	8.511	1.693	14.377	4.857		
7.386–4	8.472	1.774	14.187	4.675		
8.057–4	8.328	1.879	14.025	4.726		
8.789–4	8.147	1.889	13.730	4.732		
9.588–4	7.993	1.860	13.450	4.699		
1.046–3	7.878	1.815	13.183	4.662		
1.141–3	7.786	1.781	12.922	4.625		
1.244–3	7.708	1.758	12.664	4.596		
1.358–3	7.640	1.757	12.394	4.576	15.748	5.671
1.481–3	7.559	1.776	12.103	4.543	15.486	5.879
1.615–3	7.463	1.798	11.812	4.477	15.117	6.097
1.762–3	7.353	1.822	11.547	4.390	14.680	6.216
1.922–3	7.221	1.832	11.315	4.305	14.326	6.260
2.097–3	7.097	1.807	11.101	4.244	14.042	6.375
2.287–3	7.009	1.780	10.882	4.209	13.727	6.573
2.495–3	6.932	1.783	10.632	4.185	13.335	6.812
2.721–3	6.835	1.809	10.350	4.123	12.847	7.045
2.969–3	6.703	1.819	10.117	4.004	12.273	7.210
3.238–3	6.596	1.791	9.987	3.903	11.612	7.184
3.532–3	6.499	1.797	9.755	3.942	11.398	7.257
3.853–3	6.375	1.799	9.486	3.891	10.732	7.483
4.203–3	6.260	1.791	9.282	3.807	10.078	7.409
4.585–3	6.138	1.758	9.074	3.748	9.558	7.328
5.002–3	6.046	1.754	8.863	3.711	8.997	7.384
5.456–3	5.913	1.736	8.655	3.640	8.506	7.304
5.952–3	5.821	1.699	8.453	3.593	7.921	7.208
6.492–3	5.701	1.677	8.227	3.555	7.428	7.066
7.082–3	5.608	1.611	8.026	3.444	6.773	6.949
7.725–3	5.533	1.610	7.813	3.395	6.232	6.707
8.427–3	5.450	1.549	7.611	3.302	5.711	6.309
9.192–3	5.379	1.537	7.437	3.211	5.279	6.105
1.003–2	5.299	1.514	7.260	3.151	4.888	5.794
1.094–2	5.230	1.501	7.080	3.057	4.612	5.450
1.193–2	5.156	1.508	6.917	2.990	4.299	5.156
1.302–2	5.039	1.497	6.758	2.898	3.985	4.916
1.420–2	4.929	1.458	6.597	2.838	3.629	4.546
1.549–2	4.849	1.406	6.449	2.754	3.588	4.155
1.689–2	4.791	1.371	6.288	2.676	3.283	3.960
1.843–2	4.737	1.355	6.162	2.595	3.108	3.646
2.010–2	4.669	1.340	6.019	2.500	2.980	3.392
2.193–2	4.598	1.320	5.912	2.431	2.875	3.148
2.392–2	4.528	1.306	5.809	2.366	2.797	2.923
2.609–2	4.468	1.290	5.704	2.311	2.702	2.738
2.846–2	4.391	1.298	5.593	2.260	2.611	2.533
3.105–2	4.319	1.253	5.491	2.213	2.568	2.333
3.387–2	4.263	1.240	5.382	2.176	2.501	2.203
3.694–2	4.206	1.248	5.274	2.130	2.445	2.061
4.030–2	4.100	1.258	5.160	2.108	2.358	1.922
4.396–2	4.010	1.216	5.030	2.057	2.315	1.775
4.795–2	3.946	1.186	4.912	2.009	2.280	1.634
5.231–2	3.886	1.154	4.802	1.963	2.253	1.532
5.706–2	3.818	1.141	4.702	1.900	2.217	1.425
6.224–2	3.734	1.101	4.601	1.829	2.197	1.319
6.790–2	3.700	1.065	4.527	1.812	2.177	1.247
7.407–2	3.650	1.044	4.427	1.753	2.156	1.172
8.079–2	3.612	1.032	4.348	1.712	2.115	1.111
8.813–2	3.558	1.032	4.263	1.677	2.093	1.035
9.614–2	3.489	1.005	4.129	1.649	2.059	0.972
1.049–1	3.447	0.979	4.084	1.593	2.038	0.921
1.144–1	3.412	0.967	4.008	1.535	2.013	0.854
1.248–1	3.373	0.979	3.971	1.534	1.997	0.814
1.361–1	3.295	0.997	3.857	1.555	1.964	0.769
1.485–1	3.205	0.976	3.723	1.519	1.931	0.729
1.620–1	3.126	0.937	3.599	1.453	1.901	0.671
1.767–1	3.070	0.884	3.509	1.339	1.885	0.621
1.927–1	3.026	0.853	3.468	1.278	1.889	0.575
2.102–1	3.000	0.804	3.425	1.178	1.857	0.559
2.293–1	2.990	0.771	3.443	1.144	1.842	0.484
2.502–1	2.973	0.774	3.418	1.148	1.842	0.457
2.729–1	2.933	0.770	3.366	1.142	1.831	0.430
2.977–1	2.897	0.760	3.325	1.123	1.828	0.399
3.247–1	2.860	0.754	3.268	1.122	1.820	0.374
3.542–1	2.827	0.754	3.216	1.106	1.816	0.356
3.864–1	2.784	0.737	3.168	1.100	1.803	0.328
4.215–1	2.754	0.732	3.123	1.081	1.799	0.309
4.598–1	2.719	0.725	3.076	1.075	1.793	0.287
5.015–1	2.685	0.720	3.040	1.075	1.793	0.270
5.471–1	2.654	0.713	2.992	1.077	1.792	0.257
5.968–1	2.616	0.714	2.945	1.084	1.788	0.244
6.510–1	2.576	0.715	2.891	1.093	1.783	0.235
7.101–1	2.541	0.710	2.840	1.097	1.782	0.224
7.746–1	2.507	0.707	2.785	1.109	1.779	0.214
8.450–1	2.477	0.705	2.728	1.117	1.779	0.208
9.217–1	2.441	0.706	2.677	1.132	1.778	0.202
1.005+0	2.412	0.707	2.612	1.152	1.778	0.198
1.097+0	2.378	0.710	2.545	1.166	1.778	0.195
1.196+0	2.349	0.716	2.477	1.181	1.779	0.195
1.305+0	2.314	0.730	2.406	1.195	1.780	0.198
1.424+0	2.271	0.737	2.335	1.216	1.779	0.200
1.553+0	2.235	0.739	2.246	1.241	1.781	0.203
1.694+0	2.203	0.751	2.146	1.249	1.786	0.212
1.848+0	2.165	0.766	2.049	1.248	1.790	0.224
2.016+0	2.123	0.782	1.952	1.242	1.794	0.240
2.199+0	2.080	0.799	1.852	1.232	1.798	0.264
2.398+0	2.033	0.818	1.749	1.213	1.795	0.295
2.616+0	1.980	0.839	1.647	1.181	1.784	0.330
2.854+0	1.919	0.860	1.552	1.139	1.765	0.365
3.113+0	1.851	0.878	1.466	1.093	1.739	0.400
3.396+0	1.776	0.891	1.383	1.046	1.706	0.433
3.705+0	1.694	0.897	1.301	0.994	1.665	0.462
4.041+0	1.607	0.894	1.221	0.935	1.619	0.485
4.408+0	1.512	0.889	1.146	0.862	1.568	0.501
4.808+0	1.392	0.854	1.080	0.778	1.515	0.504
5.245+0	1.289	0.764	1.041	0.679	1.469	0.504
5.722+0	1.235	0.654	1.021	0.596	1.422	0.494
6.241+0	1.225	0.553	1.011	0.506	1.381	0.478
6.808+0	1.256	0.463	1.047	0.424	1.366	0.463
7.427+0	1.326	0.428	1.097	0.386	1.346	0.465
8.101+0	1.371	0.450	1.135	0.413	1.321	0.478
8.837+0	1.386	0.509	1.103	0.423	1.279	0.494
9.640+0	1.351	0.560	1.074	0.420	1.231	0.495
1.052+1	1.293	0.601	1.043	0.400	1.177	0.498
1.147+1	1.214	0.622	1.012	0.379	1.116	0.484
1.251+1	1.127	0.617	0.985	0.346	1.061	0.454
1.365+1	1.040	0.586	0.966	0.312	1.015	0.415
1.489+1	0.969	0.530	0.953	0.279	0.982	0.370
1.624+1	0.921	0.466	0.943	0.247	0.961	0.329
1.772+1	0.888	0.403	0.936	0.218	0.944	0.293
1.933+1	0.868	0.341	0.930	0.191	0.931	0.256
2.108+1	0.861	0.283	0.922	0.160	0.922	0.221
2.300+1	0.861	0.232	0.921	0.119	0.917	0.189
2.508+1	0.866	0.186			0.914	0.157
2.736+1	0.874	0.144			0.914	0.123
2.985+1	0.892	0.100			0.925	0.086
3.090+1	0.910	0.081			0.939	0.069

have decided to evaluate them by using a computer simulation. The extinction coefficient K has been perturbed by Gaussian noise, which has a standard deviation similar to the experimental errors reported by Colangeli et al. (1995). By using the 'new' extinction coefficient, we have calculated the corresponding sets of A, n, k and the index γ with the algorithms described above. From a statistical series of these quantities, we have derived the mean square errors. The typical errors of n and k are, respectively, 2–4 and 7–10 per cent in the far-IR, 1–2 and 4–5 per cent in the EUV, and 0.5–2 and 2–3 per cent for the rest of the energies. We have also found the estimates of $\gamma_{\rm fit}$ for the low-energy extrapolations: 0.008 ± 0.001 (ACAR), -0.224 ± 0.002 (BE) and 0.069 ± 0.002 (ACH2).

In Fig. 3, the resultant optical constants of the amorphous carbon samples considered are compared with those calculated by using various MCDE models, and with those obtained by other authors. One can see that the optical

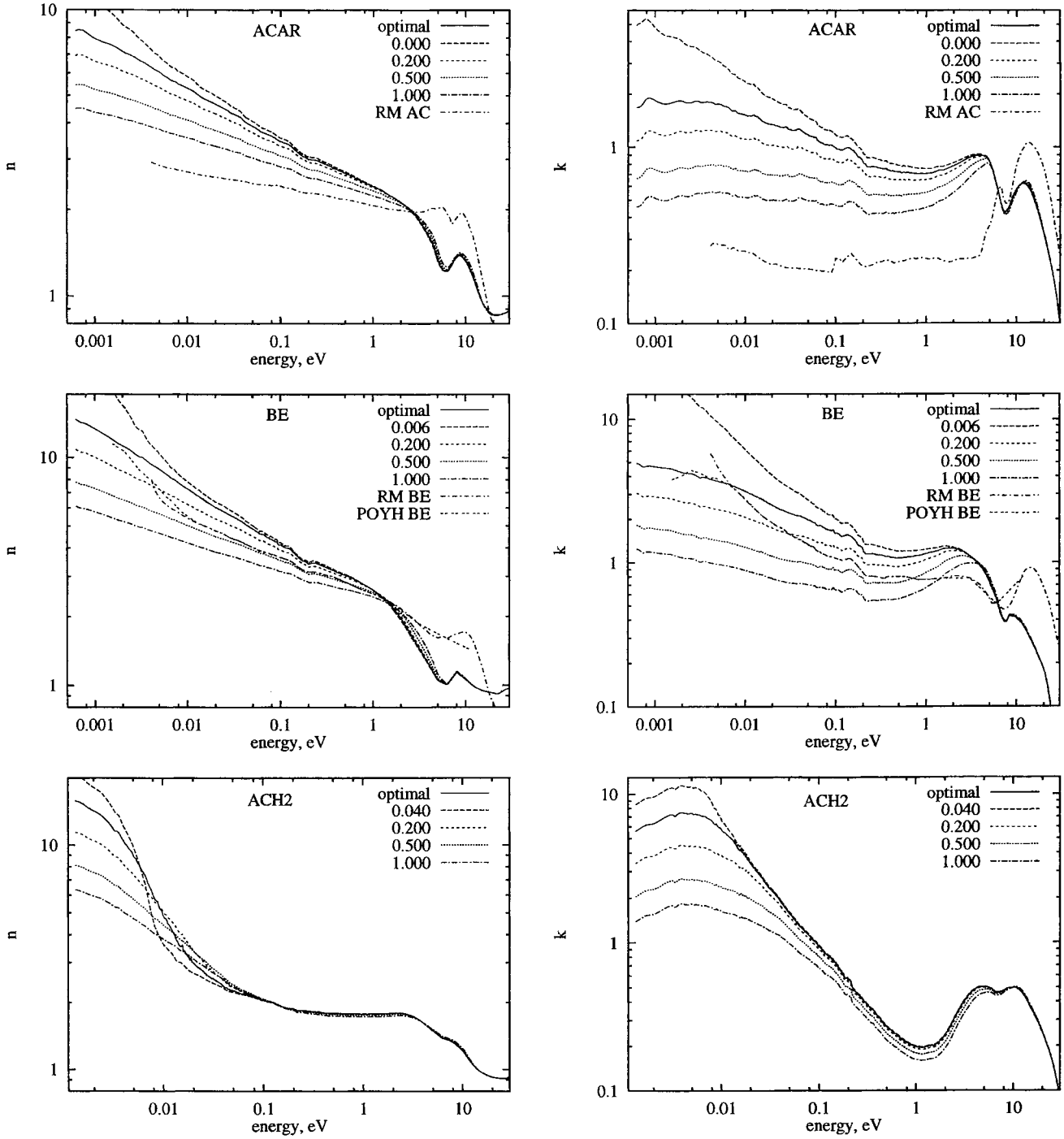

Figure 3. The optical constants of the amorphous carbon samples considered, obtained by using various MCDE models. The curves are labelled by a number corresponding to the percolation strength g_o. The results of Rouleau & Martin (1991) [RM] for the AC and BE grains (CDE models) and Preibisch et al. (1993) [POYH] for the BE grains are also shown.

constants do not depend on the model (g_o) for energies >1–2 eV for ACAR and BE and >0.1 eV for ACH2. We note differences between our results and previous results of Rouleau & Martin (1991) for AC and BE grains, and Preibisch et al. (1993) for BE, especially in the UV. We attribute them to the use of the new data sets of Colangeli et al. (1995), which are more extended in energy with respect to the data of Bussoletti et al. (1987), mainly used by Rouleau & Martin (1991) and Preibisch et al. (1993). The new data cover the strong far-UV bump at 80–95 nm which was lacking in the previous data. Moreover, Rouleau & Martin (1991), for the region 4–30 eV, used the ε_i data reported by Fink et al. (1984) for carbon samples that were different from ACAR and BE, so this inevitably influenced the optical constants.

5 CONCLUSIONS

In this paper we have presented a first approach towards deriving the optical constants for amorphous carbon grains starting from laboratory extinction data.

We have shown that the physically correct simulation of clustering by the traditional CDE model of Bohren & Huffman (1983) is not applicable to the new amorphous carbon extinction data of Colangeli et al. (1995). This conclusion is independent of the adopted low-energy extrapolation.

However, we have proposed and used in our calculations a modified CDE model (MCDE) which allows one to take into account the effect of percolation of the analysed amorphous carbon clusters through the parameter g_o, interpreted as a percolation strength. Following from the g_o estimates by Stognienko et al. (1995) and the uncertainties of the experimental data used, we have derived the optical constants together with an estimate of their errors.

ACKNOWLEDGMENTS

Professor Bruce Draine is warmly thanked for drawing our attention to the papers of D. A. Verner and D. G. Yakovlev concerning partial photoionization cross-sections of the carbon atom. It is a pleasure to acknowledge helpful discussions with Andrzej Strobel, Jacek Krełowski and Walter Wegner. We also thank Dr Volker Ossenkopf, the referee, for useful comments and suggestions which helped to improve the paper. The main calculations have been performed with a Sun SPARC station 5 bought from grant No. MEN/NSF-94-196 of the US–Polish Maria Skłodowska-Curie Joint Fund II. This work has partially been supported by ASI, MURST and CNR research contracts.

REFERENCES

Aanestad P., 1995, ApJ, 443, 653
Anders E., Zinner E., 1993, Meteoritics, 28, 490
Blanco A., Bussoletti E., Colangeli L., Fonti S., Stephens J., 1991, ApJ, 382, L97
Blanco A., Bussoletti E., Colangeli L., Fonti S., Mennella V., Stephens J., 1993, ApJ, 406, 739
Bohren C. F., Huffman D. R., 1983, Absorption and Scattering of Light by Small Particles. Wiley-Interscience, New York
Bussoletti E., Colangeli L., Borghesi A., Orofino V., 1987, A&AS, 70 257
Cardelli J. A., Mathis J. S., Ebbets D. C., Savage B. D., 1993, ApJ, 402, L17
Colangeli L., Mennella V., Blanco A., Fonti S., Bussoletti E., Gumlich H. E., Mertins H. C., Jung Ch., 1993, ApJ, 418, 435
Colangeli L., Mennella V., Palumbo P., Rotundi A., Bussoletti E., 1995, A&AS, 113, 561
Czyzak S. J., Santiago J. J., 1973, Ap&SS, 23, 443
Donn B., Hecht J., Khanna R., Nuth J., Strand D., Anderson A. B., 1981, Surface Sci., 106, 576
Draine B. T., 1988, ApJ, 333, 848
Draine B. T., Flatau P. J., 1994, J. Opt. Soc. Am. A, 11, 1491
Fink J., Müller-Heinzerling Th., Pflüger J., Sheerer B., Dischler B., Koidl P., Bubenzer A., Sah R. E., 1984, Phys. Rev. B, 30, 4713
Hamid A.-K., Ciric I. R., Hamid M., 1990, Can. J. Phys., 68, 1419
Hecht J., 1986, ApJ, 305, 817
Hinsen K., Felderhof B. U., 1992, Phys. Rev. B, 46, 12955
Kim S.-H., Martin P. G., Hendry P. D., 1994, ApJ, 422, 164
Ku J. C., Felske J. D., 1986, J. Opt. Soc. Am. A, 3, 617
Landau l. D., Lifshits E. M., Pitaevskii L. P., 1984, Electrodynamics of Continuous Medium. Pergamon, Oxford
Laor A., Draine B. T., 1993, ApJ, 402, 441
Mathis J. S., Rumpl W., Nordsieck K. H., 1977, ApJ, 217, 425
Mennella V., Colangeli L., Blanco A., Bussoletti E., Fonti S., Palumbo P., Mertins H. C., 1995a, ApJ, 444, 288
Mennella V., Colangeli L., Bussoletti E., Monaco G., Palumbo P., Rotundi A., 1995b, ApJS, 100, 149
Mennella V., Colangeli L., Bussoletti E., Merluzzi P., Monaco G., Rotundi A., 1995c, Planet. Space Sci., 43, 1217
Ossenkopf V., 1991, A&A, 251, 210
Ott U., 1993, Nat, 364, 25
Preibisch Th., Ossenkopf V., Yorke H. W., Henning Th., 1993, A&A, 279, 577
Rouleau F., Martin P. G., 1991, ApJ, 377, 526
Sorrell W. H., 1990, MNRAS, 243, 570
Stephens J. R., 1980, ApJ, 237, 450
Stognienko R., Henning Th., Ossenkopf V., 1995, A&A, 296, 797
Verner D. A., Yakovlev D. G., 1995, A&AS, 109, 125
Verner D. A., Yakovlev D. G., Band I. M., Trzhaskovskaya M. B., 1993, At. Data Nucl. Data Tables, 55, 233